Study of rapid thermal annealing effect on CdZnO thin films grown on Si substrate

L. Li, Z. Yang, Z. Zuo, J. Y. Kong, and J. L. Liu[a)]
Department of Electrical Engineering, Quantum Structures Laboratory, University of California, Riverside, California 92521

(Received 14 October 2009; accepted 8 March 2010; published 7 April 2010)

CdZnO thin films were grown on Si (100) substrates by plasma-assisted molecular beam epitaxy. As-grown samples show near band edge emissions at 1.87, 2.03, and 2.16 eV, respectively, while the emission peak energy dramatically increases to up to ultraviolet region with increasing rapid thermal annealing temperature. Room temperature photoluminescence (PL), and temperature dependent PL show phase separations in the samples after the annealing process. Secondary ion mass spectroscopy measurements show redistribution of Cd in the as-annealed sample, which is believed to be the reason of PL peaks shift. © *2010 American Vacuum Society.* [DOI: 10.1116/1.3374435]

ZnO is a potential candidate for ultraviolet/blue light emitting diodes and laser diodes (LDs) applications due to its superior properties such as large exciton binding energy of 60 meV at room temperature. The band gap of ZnO can be wider by alloying Mg into ZnO,[1] while it can also be extended to green region and even longer wavelength by alloying it with Cd.[2–4] Therefore, CdZnO is a promising material for potential visible light optoelectronic applications, such as green light emitting diodes and laser diodes, photodetectors, etc. The effect of RTA on the stability of CdZnO needs to be clarified for future reliable device application because high temperature annealing is indispensable in dopant activation[5–8] and device contact formation[9–12] of ZnO-based devices. There have been some studies on the thermal stability of CdZnO quantum well structures with relatively low Cd concentration.[13,14] In this article, CdZnO thin films with large Cd content were grown on Si substrates by molecular beam epitaxy (MBE). The effect of rapid thermal annealing (RTA) on the samples was studied and reported in detail.

CdZnO thin films were grown by plasma-assisted MBE on Si(100) substrates. Elemental Zn (6*N*) and Cd (6*N*) heated by effusion cells were used as zinc and cadmium sources. Oxygen (5*N*) plasma generated by a radiofrequency plasma generator was used as the oxygen source. The samples were grown at very low growth temperatures (below 200 °C) to achieve large Cd incorporation. The effusion cell temperatures varied from 330 to 350 °C for Zn and from 280 to 310 °C for Cd in order to tune the Zn and Cd flux, hence achieve different Zn/Cd ratios. X-ray diffraction (XRD) was performed in θ-2θ geometry with a 0.1° resolution to study the crystal structure. The CdZnO samples were subjected to RTA in nitrogen ambient for 1 min at different temperatures from 300 to 900 °C to investigate the property changes after RTA process. Photoluminescence (PL) measurements were carried out using a home-built PL system, with a 325 nm He–Cd laser as excitation source and a photomultiplier tube behind the monochrometer as detector.

Table I summarizes the RT PL emission peak positions of as-grown samples A–C and the samples after RTA at different temperatures. The peak shift has been observed after annealing. For example, as-grown sample A shows near band edge (NBE) emission at 664 nm, while it evolves into two peaks at 392 and 420 nm after 900 °C RTA. NBE emission peak of sample B is centered at 610 nm in the as-grown sample, which evolves into two peaks at 385 and 425 nm after 900 °C RTA. NBE emission peak of sample C shifts from 572 to 445 nm after 900 °C RTA.

The RT PL spectra of samples A–C before and after RTA are shown in Figs. 1(a)–1(c) in logarithmic scale. All samples were subjected to RTA at 300, 500, 700, 800, and 900 °C for 1 min, respectively. PL emissions of each sample at different annealing temperatures were taken by digital camera and are shown in Figs. 2(a)–2(c). The emissions of sample A cover from red to near ultraviolet as shown in the pictures, while the emissions of sample B and sample C cover from orange to violet and from yellow to blue, respectively. As shown in Fig. 1(a), the NBE emission of sample A evolves from one peak to two dominant peaks with the peak positions at higher energies after 700 °C RTA. The two peaks further evolve into one dominant peak with a weak shoulder when annealing temperature reaches 800 °C and higher. Sample B also shows similar evident NBE emission peak evolution after annealing process.

To further study the effect of RTA process on the sample and clarify the origins of the peak shifts during the RTA process, XRD measurements were carried out on as-grown samples A–C and 800 °C annealed samples A–C, respectively. Temperature dependent PL measurements and secondary ion mass spectroscopy (SIMS) measurements were also carried out on the as-grown sample C and 800 °C annealed sample C. The temperature dependent PL results are shown in Figs. 3(a) and 3(b), respectively. The PL emission of as-grown sample is dominated by one single peak from 9 to 300 K. It shows single phase in the as-grown sample C. However, after 800 °C RTA process, PL emission of the sample C

[a)]Author to whom correspondence should be addressed; electronic mail: jianlin@ee.ucr.edu

TABLE I. Room temperature PL peak energy (eV) of as-grown samples A–C, and their room temperature PL peak energy after different temperatures RTA. All annealing time is 1 min.

	As-grown	300 °C	500 °C	700 °C	800 °C	900 °C
Sample A	1.87	1.98	2.02	2.34/2.99	2.73/3.08	2.95/3.16
Sample B	2.03	2.03	2.19	2.39	2.56/3.04	2.92/3.22
Sample C	2.17	2.16	2.19	2.29	2.48	2.79

shows two peaks with relatively similar strength at low temperature. Although they gradually merged to one peak, shoulders are evident at the right hand side of the peaks with increasing temperature. It suggests that RTA process also results in two emission peaks, i.e., phase separation to sample C, very similar to what has happened to the samples A and B.

$\theta/2\theta$ XRD measurement results of as-grown samples A–C and samples A–C after 800 °C RTA are shown in Figs. 4(a)–4(c), respectively. Upper figures show XRD spectra of the as-grown samples and lower figures show XRD spectra

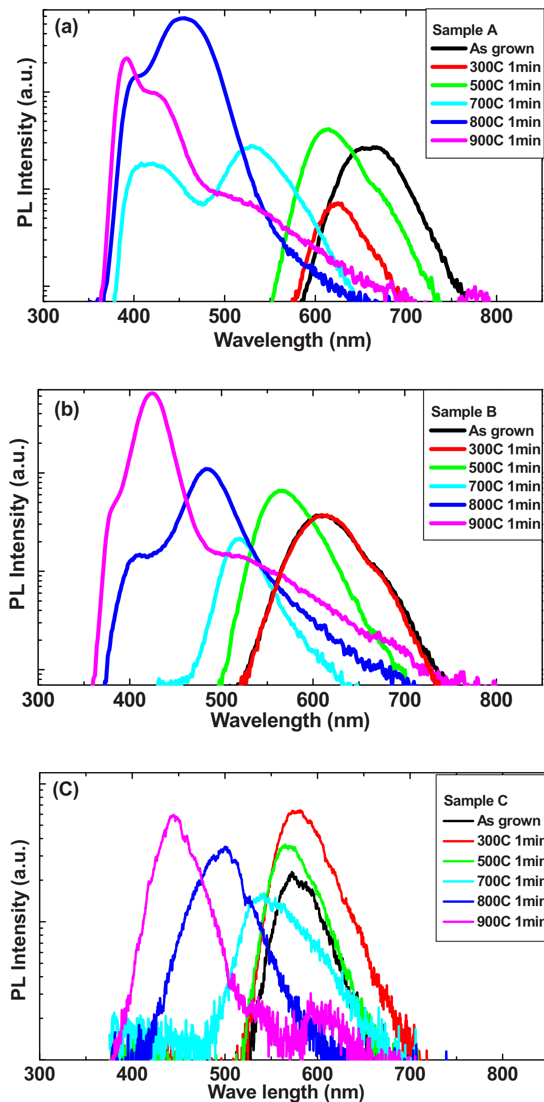

FIG. 1. (Color online) Room temperature PL spectra of samples A (a), B (b), and C (c) before and after RTA at different temperatures.

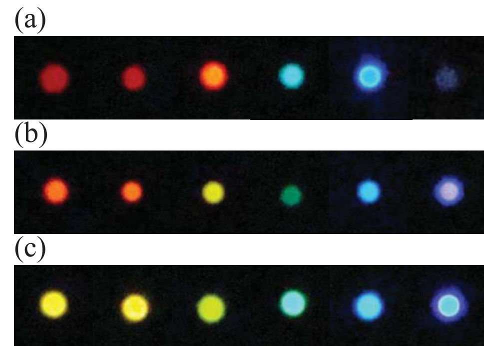

FIG. 2. (Color online) Digital camera pictures of the room temperature PL emissions of samples A (a), B (b), and C (c) before and after RTA at different temperatures. From left to right: as-grown, 300 °C RTA, 500 °C RTA, 700 °C RTA, 800 °C RTA, and 900 °C RTA. The diameter of the excitation laser beam is about 0.5 mm.

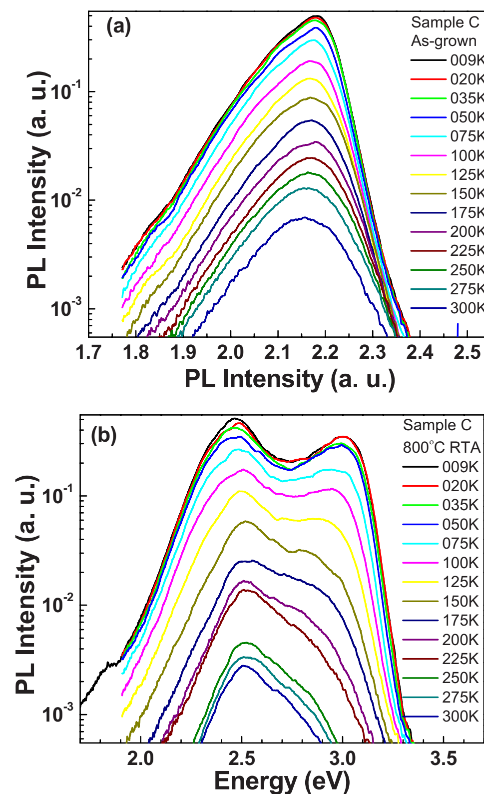

FIG. 3. (Color online) Temperature dependent PL spectra from 9 to 300 K of as-grown sample C (a), and sample C after 800 °C RTA (b).

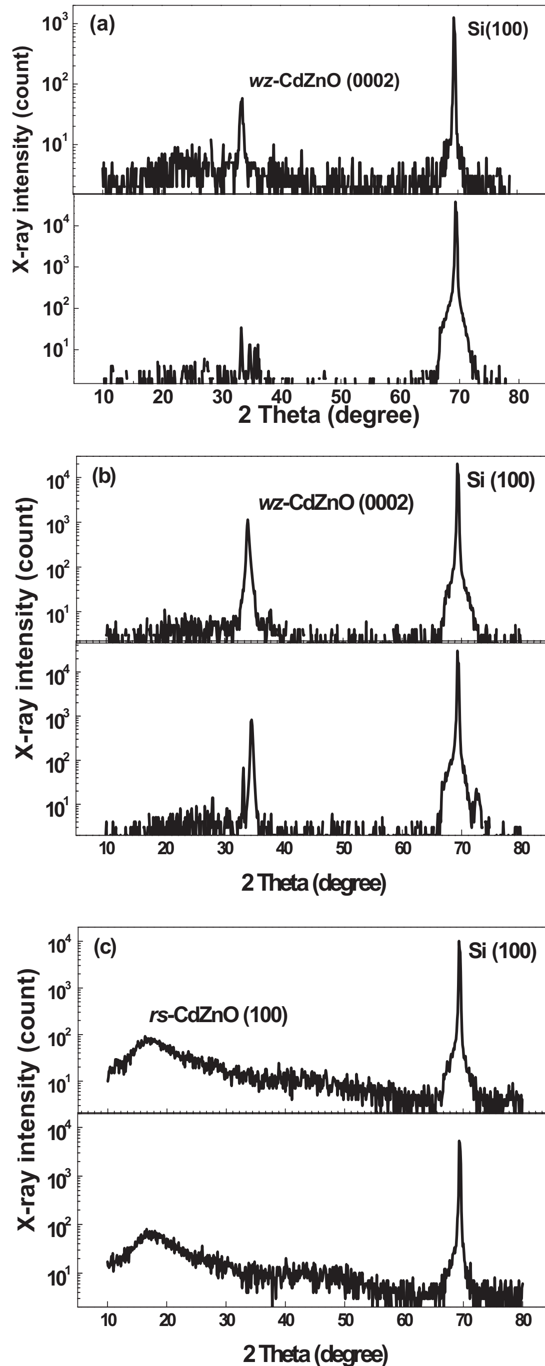

FIG. 4. XRD measurements of sample A (a), sample B (b), and sample C (c) before (upper) and after 800 °C RTA (lower).

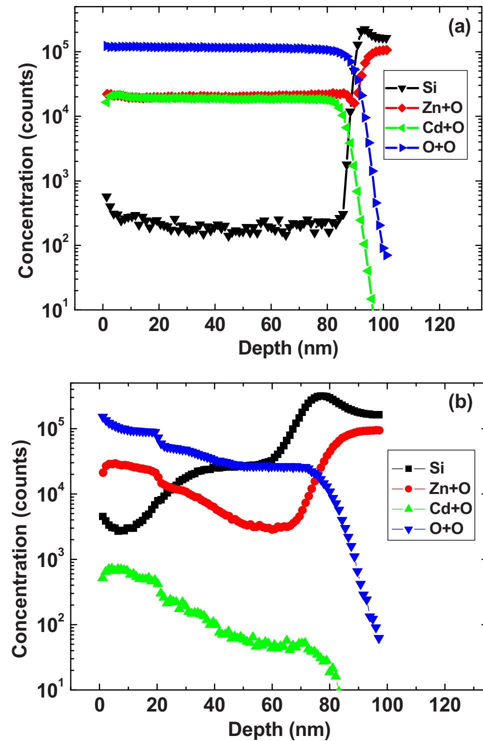

FIG. 5. (Color online) SIMS measurements of as-grown sample C (a) and sample C after RTA at 800 °C (b).

of the samples after 800 °C RTA, respectively. Samples A and B are dominated by wurtzite CdZnO (0002) peak before and after RTA, while sample C is dominated by rocksalt CdZnO (100) (Refs. 15 and 16) peak centered at around $2\theta = 17.5°$. The large full width at half maximum in sample C indicates low crystal quality as a result of low temperature growth. Compare XRD before and after RTA, it suggests that there is no evident structure change during the RTA process in all three samples.

Figures 5(a) and 5(b) show the SIMS measurement results of as-grown sample C and sample C after 800 °C RTA, respectively. The as-grown sample exhibits even distribution of Zn, O, and Cd from the surface of the thin film to the substrate. The Cd concentration is at a relatively high level although SIMS data were not calibrated to know the exact mole fraction. While after 800 °C RTA, profile of Cd dramatically changes compared to as-grown sample, as shown in Fig. 5(b). The change in Cd concentration may be due to the redistribution during the RTA. Cd could redistribute between the Cd-rich and Cd-poor regions inside the film during the annealing process. Regions with higher Cd concentration dominate the PL emission in as-grown and low temperature annealed samples, while regions with less Cd concentration dominate after high temperature annealing process.[17] Especially when the morphology of the film is nanograins, the Cd could be affiliated to the grain boundaries, which are metastable and are very possible to redistribute during high temperature annealing process. There is also Si signal detected after 800 °C RTA. It may come from Si/ZnO interdiffusion after high temperature annealing process.[18,19] Alternatively, it could come from the cracks formed on the thin film due to thermal expansion during RTA.

In summary, CdZnO samples with large Cd content were grown on Si substrates. The NBE emissions of the samples dramatically shift to higher energy with increasing RTA temperature. The PL emissions cover red to ultraviolet region. Room temperature PL and temperature dependent PL reveal that phase separations happen during the annealing process,

while SIMS measurements show Cd redistribution after annealing, which explains band gap change in CdZnO.

ACKNOWLEDGMENT

This work was supported by DOE under Grant No. DE-FG02-08ER46520.

[1]A. Ohtomo *et al.*, Appl. Phys. Lett. **72**, 2466 (1998).
[2]T. Makino, Y. Segawa, M. Kawasaki, A. Ohtomo, R. Shiroki, K. Tamura, T. Yasuda, and H. Koinuma, Appl. Phys. Lett. **78**, 1237 (2001).
[3]Ü. Özgür *et al.*, J. Appl. Phys. **98**, 041301 (2005) and reference therein.
[4]S. Shigemori, A. Nakamura, J. Ishihara, T. Aoki, and J. Temmyo, Jpn. J. Appl. Phys., Part 2 **43**, L1088 (2004).
[5]F. X. Xiu, Z. Yang, L. J. Mandalapu, D. T. Zhao, J. L. Liu, and W. P. Beyermann, Appl. Phys. Lett. **87**, 152101 (2005).
[6]F. X. Xiu, Z. Yang, L. J. Mandalapu, D. T. Zhao, and J. L. Liu, Appl. Phys. Lett. **87**, 252102 (2005).
[7]F. X. Xiu, Z. Yang, L. J. Mandalapu, J. L. Liu, and W. P. Beyermann, Appl. Phys. Lett. **88**, 052106 (2006).
[8]F. X. Xiu, Z. Yang, L. J. Mandalapu, and J. L. Liu, Appl. Phys. Lett. **88**, 152116 (2006).
[9]L. J. Mandalapu, Z. Yang, F. X. Xiu, D. T. Zhao, and J. L. Liu, Appl. Phys. Lett. **88**, 092103 (2006).
[10]L. J. Mandalapu, Z. Yang, and J. L. Liu, Appl. Phys. Lett. **90**, 252103 (2007).
[11]L. J. Mandalapu, Z. Yang, S. Chu, and J. L. Liu, Appl. Phys. Lett. **92**, 122101 (2008).
[12]S. Chu, M. Olmedo, Z. Yang, J. Y. Kong, and J. L. Liu, Appl. Phys. Lett. **93**, 181106 (2008).
[13]A. V. Thompson *et al.*, Appl. Phys. Lett. **91**, 201921 (2007).
[14]S. Sadofev, S. Kalusniak, J. Puls, P. Schäfer, S. Blumstengel, and F. Henneberger, Appl. Phys. Lett. **91**, 231103 (2007).
[15]H. Liu, H. K. Mao, M. Somayazulu, Y. Ding, Y. Meng, and D. Häusermann, Phys. Rev. B **70**, 094114 (2004).
[16]C. Alétru, G. N. Greaves, and G. Sankar, J. Phys. Chem. B **103**, 4147 (1999).
[17]F. Bertram, S. Giemsch, D. Forster, J. Christen, R. Kling, C. Kirchner, and A. Waag, Appl. Phys. Lett. **88**, 061915 (2006).
[18]M. Jung, J. Lee, S. Park, H. Kim, and J. Chang, J. Cryst. Growth **283**, 384 (2005).
[19]X. Q. Zhao *et al.*, Appl. Surf. Sci. **255**, 4461 (2009).